# Oriented biotite inclusions in diamond coat

NATURAL diamonds contain mineral inclusions that represent valid samples of the upper mantle of the Earth (where diamond crystallisation occurred) provided that they are totally enclosed within the diamond and do not derive from material later infiltrating via cracks. Inclusions satisfying this condition, and which are also of macroscopic size (diameters > 100 μm, say), have been studied over many years. Some important reports and reviews of this work are by Williams (1932), Harris (1968), Meyer and Boyd (1972), Meyer and Tsai (1976) and Harris and Gurney (1979).

Much less is known concerning microscopic inclusions. A striking manifestation of such is in diamond 'coat'. A significant fraction of natural diamonds are of the 'coated' variety. These have a clear octahedral core (often of gem quality) completely enveloped by a coat shell in which the diamond matrix is densely populated by sub-micrometre-size non-diamond bodies (Kamiya and Lang, 1965; Seal, 1966; Navon et al., 1988).

To discover the composition of and (if possible) mineralogically identify such bodies individually requires the resolution of analytical electron microscopic techniques (Lang and Walmsley, 1983; Bruley and Brown, 1989). Transmission electron microscopy, electron diffraction and energy-dispersive X-ray spectroscopy combined have identified apatite inclusions in diamond coat (Lang and Walmsley, 1983). Here we report the identification of biotite mica in diamond coat, and a preferred orientation relationship between the sub-micrometre-size mica crystallites and their diamond host.

We have studied coated diamonds from Zaïre, sawing slices parallel to (100) and (110), mechanically polishing them down to about 50 μm thickness and, finally, ion-beam milling chosen coat-containing pieces to a thickness of ≤1 μm for transmission electron microscopy. The thinned specimen foils show numerous holes (diameters ≈0.1–1.0 μm) from which the contents have been lost, but a small percentage of the opened cavities (which become rounded by ion-beam erosion) retain some solid non-diamond substance.
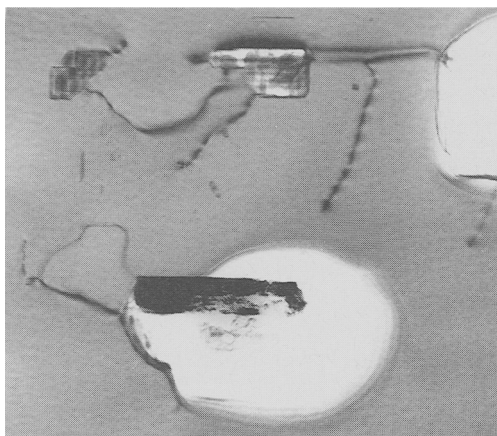
The micrograph, Fig. 1, shows both opened



FIG. 1. Transmission electron micrograph (bright-field) of thinned diamond coat showing uneroded, inclusion-containing cavities bounded by diamond {111} facets (top and top left), larger, eroded (open) cavities (top right and lower centre), and dislocations. In the lower-central cavity a single biotite crystallite is silhouetted, its less eroded parts appearing dark by diffraction contrast. The (100)-orientation diamond foil has been tilted 35° to give diamond [211] zone-axis diffraction conditions. Biotite (001) and diamond ($\bar{1}$11) planes are parallel; their normals lie vertical in the image. Field width 1 μm, long dimension of biotite crystallite 0.34 μm.

and unopened cavities, with dislocations running between cavities or outcropping at the foil surfaces. The lower-central cavity contains a mica crystallite, its elongated rectangular silhouette being typical of such crystals viewed parallel to their cleavage planes. At its upper left end it remains protected by intimate contact with the diamond matrix. There the close flatness of its (001) surface, parallel to a diamond octahedral plane, is clearly evident in this edge-on view. The diffraction pattern of this particle, Fig. 2, demonstrates an exact simple orientation relationship with the matrix, but in this case double diffraction, giving ghost rows of spots, complicates the pattern. A clearer mica diffraction pattern is shown in Fig. 3, where slight misorientation off

the mica (001) ‖ diamond (111) relationship avoids confusion by double diffraction. Inclusion morphology similar to that in Fig. 1, accompanied by diffraction patterns similar to those in Figs. 2 and 3, have been observed in some dozens of cases. Unit cell dimensions and symmetry accord with a monoclinic mica having $1M$ stacking of unit structures (Smith and Yoder, 1956), with lattice parameters $a = 0.53$, $b = 0.92$ nm and basal plane spacing $c \sin\beta = 1.02$ nm. Rotation of the specimen setting of Fig. 2 by 30° about the normal to the mica (001) gave the [310] zone axis diffraction pattern expected with these cell parameters. The diamond pattern serves to calibrate interplanar spacing measurements, which Fig. 2 gives to an accuracy of about ±1% (and about ±1° for β), and Fig. 3 to ±0.5%. About two-thirds of the diffraction patterns photographed show some streaking between spots in general rows parallel to the mica reciprocal lattice vector $c^*$, evidence of stacking disorder of unit layers.

Energy dispersive X-ray spectroscopy (EDS) of the particle in Fig. 1 was complicated by P and Ca peaks, probably from apatite in the same cavity, but inconspicuous in Fig. 1 through lack of



Fig. 3. Diffraction pattern of a biotite inclusion oriented with its $a$-axis parallel to the electron beam. Biotite reflections fall on orthogonal $0, 2k, l$ net corresponding to $b = 0.918$ nm, $c \sin\beta = 1.015$ nm. Biotite (001) tilted off diamond octahedral plane by about 1.4°.
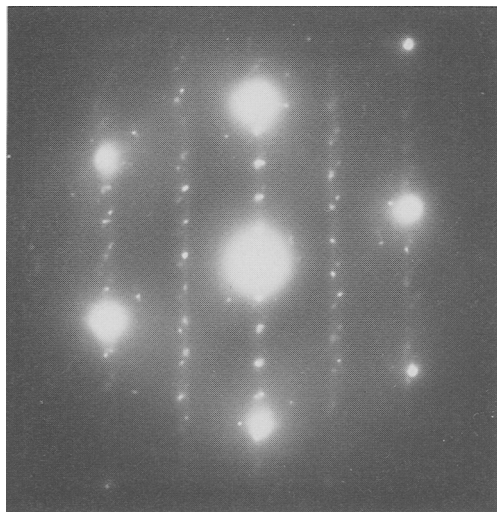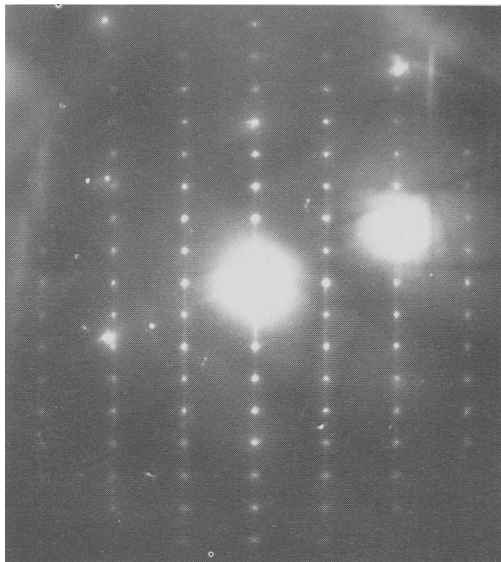


Fig. 2. Selected-area electron diffraction pattern from biotite crystallite shown in Fig. 1 including some immediately adjacent diamond matrix. Specimen rotated relative to its setting in Fig. 1 by 30° about the common normal to diamond ($\bar{1}11$) and biotite (001) so as to produce diamond [110] and biotite [110] zone-axis diffraction patterns simultaneously. Diamond [001] points to upper left, rotated 54.74° from vertical. Strong diamond reflections above and below central direct beam are $\bar{1}11$ and $1\bar{1}\bar{1}$, respectively; biotite 00$l$ reflections lie on the same median vertical line, and $hh\bar{l}$ reflections on other vertical rows.

diffraction contrast. Moreover, loss of image contrast and diffraction pattern quality after the electron beam had been focused on the mica particle rendered its analysis doubtful. To keep electron-beam damage low, an EDS spectrum was acquired rapidly from another particle giving the same diffraction pattern, located in another cavity, and is shown in Fig. 4. Peak areas in Fig. 4 were converted to element abundance ratios by comparison with the EDS spectrum of a thin biotite specimen whose element abundance ratios had been found by well-calibrated electron-probe X-ray spectroscopic analysis. The analysis of the diamond-coat particle differs from the biotite composition range (Deer et al., 1966; Radoslovich and Norrish, 1962) only by excess Si, which is attributed to presence in the cavity of another, Si-rich phase (biotite generally coexists with other phases in cavities where it is found). The insensitivity of the EDS to elements with $Z \leq 11$ (Na, F, O), plus the excess Si, preclude fitting the particle composition to a standard mica chemical formula. The findings are best stated simply as cation ratios: Mg 0.86, Al 0.92, Si 4.74, K 1.0, Ti 0.3, Fe 0.86. The minor Cl content has not been quantified. A small (but statistically significant) enhancement of the potassium $K\beta$ peak is explicable by overlap with Ca-$K\alpha$, with a Ca/K ratio of 3–5%. It is on the basis of the low Mg/Fe ratio of ≈1,

well below the value 2, that this particle (and others having similar unit cell dimensions) are identified as biotite (Deer *et al.*, 1966). The occurrence of biotite as a primary inclusion (syngenetic or pre-syngenetic) in diamond was reported in the classic work of A. F. Williams (1932) and again by Giardini *et al.* (1974). The latter workers recovered 3 flakes of brown mica (0.1 × 0.1 mm) from the fragments of 39 crushed small African diamonds previously cleaned and microscopically checked as crack-free. X-ray diffraction and electron-probe X-ray spectroscopy identified the mica as biotite (Mg/Fe = 0.65). The present work identifies biotite crystallites *in situ* in diamond coat. Furthermore, it is found that a preferred orientation with respect to the diamond matrix is exhibited by about half the biotite crystals studied; this is, specifically, biotite (001) parallel to a diamond octahedral plane, say ($\bar{1}$11), with diamond [110] parallel to biotite [110] or to an equivalent direction (*a* or [1$\bar{1}$0]) in a single sheet of $(Si,Al)_2O_5$ rings. With this relationship, the inter-centre vectors of the $(Si,Al)_2O_5$ rings in the mica lie parallel to C-C zig-zag chains in the diamond octahedral planes. the inter-centre distance, 0.53 nm, exceeds the diamond f.c.c. face diagonal, 0.504 nm, by ≈5%.
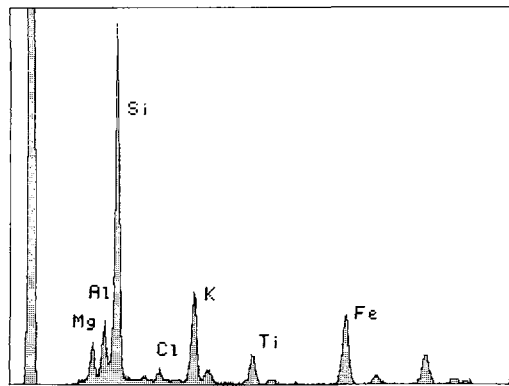
FIG. 4. Energy-dispersive X-ray spectrum from a particle similar to that imaged in Fig. 1. Abscissa and ordinate scales are linear in energy and in accumulated counts, respectively. Unlabelled peaks are, on left, zero-marker for the energy scale and, on right, Cu-*K* fluorescence from the copper sample holder. For potassium and elements of higher Z, the *K*α and *K*β peaks are separated, the *K*β peak having intensity 0.1 and energy 1.1 times the *K*α values.

## References

Bruley, J. and Brown, L. M. (1989) Quantitative EELS microanalysis of nanometre sized defects and inclusions in natural diamond. *Mat. Res. Soc. Symp. Proc.*, **138**, 131–6.

Deer, W. A., Howie, R. A., and Zussman, J. (1966). *An Introduction to the Rock-Forming Minerals*, Longman, London.

Giardini, A. A., Hurst, V. J., Melton, C. E., and Stormer, J. C., Jr. (1974) Biotite as a primary inclusion in diamond: its nature and significance. *Am. Mineral.*, **59**, 783–9.

Harris, J. W. (1968) The recognition of diamond inclusions—Part 1: syngenetic mineral inclusions. *Industrial Diamond Review*, **28**, 402–10.

—— and Gurney, J. J. (1979) In *The Properties of Diamond* (Field, J. E., ed.). Academic Press, London, 555–91.

Kamiya, Y. and Lang, A. R. (1965) On the structure of coated diamonds. *Phil. Mag.*, **11**, 347–56.

Lang, A. R. and Walmsley, J. C. (1983) Apatite inclusions in natural diamond coat. *Phys. Chem. Minerals*, **9**, 6–8.

Meyer, H. O. A. and Boyd, F. R. (1972) Composition and origin of crystalline inclusions in natural diamonds. *Geochim. Cosmochim. Acta*, **36**, 1255–73.

—— and Tsai, H.-M. (1976) The nature and significance of mineral inclusions in natural diamond: a review. *Minerals Sci. Engng.*, **8**, 242–61.

Navon, O., Hutcheon, I. D., Rossman, G. R., and Wasserburg, G. J. (1988) Mantle-derived fluids in diamond micro-inclusions. *Nature*, Lond., **335**, 784–9.

Radoslovich, E. W. and Norrish, K. (1962) The cell dimensions and symmetry of layer-lattice silicates. Some structural considerations. *Am. Mineral.*, **47**, 599–616.

Seal, M. (1966) Nature of diamond coat. *Phil. Mag.*, **13**, 645–8.

Smith, J. V. and Yoder, H. S. (1956) Experimental and theoretical studies of the mica polymorths. *Mineral. Mag.*, **31**, 209–35.

Williams, A. F. (1932) *The Genesis of the Diamond*, Vol. II. Ernest Benn, London.

*H. H. Wills Physics Laboratory,*
*University of Bristol, Royal Fort,*
*Tyndall Avenue, Bristol BS8 1TL, UK*

J. C. WALMSLEY*
A. R. LANG

* Present Address: *Nuclear Electric, Berkeley Nuclear*
*Laboratories, Berkeley, Gloucestershire GL13 9PB, UK*

# An unusual octahedral diamond

THIS clear and colourless diamond (0.35 cts) from the Alpheus Williams collection (Williams, 1932) on display at the Kimberley Open Mine Museum, South Africa, has been examined in the course of a study (Yacoot, 1990) of the modes of growth and consequent morphologies of some natural diamonds. There are small dodecahedra on the six vertices of the octahedron. Fig. 1a is a general view of the specimen and Fig. 1b shows one of the dodecahedra at higher magnification. Fig. 1c shows some of the unusual facets on the octahedron. From the morphology imaged by these scanning electron micrographs, one infers that the specimen has suffered dissolution: the dodecahedra are rounded and there are {110} bevels between adjacent {111} faces on the octahedron, some of the latter approximating to triangular triakisoctahedral faces $\{hhl\}$, $h > l$.

A Laue picture, taken with polychromatic synchrotron radiation (at the SERC Daresbury Laboratory, Warrington, Cheshire) which illuminated the entire specimen, showed that the dodecahedra were not mis-orientated from the octahedron and that the specimen was a single crystal. That having been established, the diamond was examined by X-ray topography (Lang, 1957, 1958; Moore, 1988) using Mo-$K\alpha_1$ radiation and the $4\bar{4}0$ reflexion ($\lambda = 0.71$ Å, $\theta_B = 34°15'$). Such a diffraction geometry produced images of crystal sections almost parallel (offset by 1°) to the $(\bar{1}11)$ plane. Fig. 1d–f shows the first three section topographs in a series of six that imaged the crystal at 0.5 mm intervals.

The topographic image through the centre of the crystal (Fig. 1f) shows incomplete growth banding in the octahedron, together with several areas of localised strain. The twelve-sided outline of the topograph is similar to a section of a rounded (diakis) rhombic dodecahedral diamond described by Moore (1973). A very dark circular region can be seen in the centre of the topograph, which is the imperfect nucleus from which crystal growth started. Other topographs in the series show more growth banding in the octahedron. Fig. 1d and e show growth bands within the dodecahedra, which appear to make re-entrant angles with another. These dodecahedra are the remnants of dissolved octahedra (Moore and Lang, 1974) on the vertices of the (major) octahedron.

The topographs show that crystal growth started from an imperfect and highly strained nucleus and the growth banding confirms that growth was on {111} planes. That some of the growth banding in the major octahedron is incomplete, being partially intersected by the six minor octahedra, suggests that dissolution occurred prior to the formation of these minor octahedra. This dissolution would have started at the major octahedron's six vertices, turning them into nucleation centres for further growth. Faceted growth then occurred in the $\langle 111 \rangle$ directions at these vertices, resulting in the formation of the six minor octahedra. Although the growth bands appear to diverge from the surfaces of the minor octahedra, independent growth did not occur towards the centre of the specimen. (If this had happened from separate centres, there would certainly have been some mis-orientation between the major and minor octahedra. The chance of six minor octahedra adhering in perfect orientation to the vertices of an octahedron is extremely unlikely.) Finally, the specimen suffered some more dissolution which